

Adaptive Region Merging Approach for Morphological Color Image Segmentation

Huang-Chia Shih and En-Rui Liu

Human-Computer Interaction Multimedia Lab., Department of Electrical Engineering
Innovation Center for Big Data and Digital Convergence
Yuan Ze University, Taoyuan 32003, Taiwan
hcshih@saturn.yzu.edu.tw

Abstract. This study we focus on the morphological-based image segmentation problem, based on the watershed pre-segmentation with color-alone feature. Based on the color mathematical morphology (MM) method, the similarity measure of merging process between neighboring pixels and regions can be performed as a ranking problem. To avoid the creation of a false color and false segmentation, a hybrid-ordering algorithm instead of vectorized and marginal ordering approaches. Unlike other ordering methods firmly the black color as the reference color to sort pixels, it creates the problem that the scope of the distance measurement is not optimum. We present an automatic reference color selection (ARCS) scheme to obtain the segmentation results more line with human visual perception. Based on a new quartile-based region merging approach, the threshold determination reacts less sensitivity to the context variations of images. To evaluate the system, four quantitative indices are utilized to compare it two typical segmentation schemes in the experiments. It shows that the result of the proposed method is robust to segment the image.

1 Introduction

Numerous segmentation methods have been proposed extensively using the primary features of image such as color and texture. In last decade, the algorithms to integrate the color and texture descriptors have attracted much attention in the research literature, e.g., model-based energy function [1], graph-based representation [2], Gaussian mixture models [3], Markov random field (MRF) [4], spatially adaptive dominant colors [5], and some well-known systems with the implicit color-texture feature integration such that JSEG [6], GRF [7], CTex [8], GSEG [9], and normalized cuts [10] have been carried out in this area. Additional information on color-texture descriptors can be found in review publications [11]. Nevertheless, in order to trade-off between segmentation accuracy and computational cost of the system, many research efforts have taken place regarding the color-alone [12]-[14] and texture-along [15]-[17] image information.

In recent years mathematical morphology (MM) [18]-[20] has been widely used in image processing. Compared with the single dimensional image (e.g. binary and grayscale), there is no standard ordering mechanism for color feature vectors. In re-

cent years, a great amount of literatures report the sequential ordering approaches of the color morphology, which can be categorized into four fundamental modes: Marginal-ordering (M-ordering) [21], Reduced-ordering (R-ordering) [22], Conditional-ordering (C-ordering) [23], and Partial-ordering (P-ordering) [24].

In the present study we proposed an improved color ordering method called CRC-ordering. Similar to [25] that integrated the R-ordering and C-ordering methods in ranking determination, but unlike other methods firmly using conventional Euclidean distance with black color as the reference color to sort pixels [26], it creates the problem that the scope of the distance measurement is not optimum. Therefore, we present an automatic reference color selection (ARCS) mechanism using the HSI distance measurement. It allows dealing with diverse color models, while avoiding the ambiguous situation of ranking comparisons in color vectors. Finally, we present a novel automatic threshold determination method to region merging process using the quartile analysis. To demonstrate the feasibility of the new region merging algorithm, we compared with the performance in experiments section.

2 Color Basis and Ranking Algorithm

2.1 Color representations and color distances

The typical color model used in image processing is a Red-Green-Blue (RGB) representation. However, the RGB color model suffers from an intrinsic drawback, its high correlation between color channels. Furthermore, it is unable to obtain the original intensity information of the image in order to reduce the computation burden in the image acquisition phase. To overcome this problem, we employed the HSI (Hue-Saturation-Intensity) color model. It is not only more coherence with the characteristics of human perception, but also more appropriate for the regional split-and-merge operation in image segmentation.

The HSI color model is designed as a cylindrical-coordinate representation with different scales for each color component. In practice the HSI distance is used to measure the distinction between the testing color and the reference color. Let's suppose that there are two color points in the HSI color space, and that they are represented by $p(H_p, S_p, I_p)$ and $q(H_q, S_q, I_q)$ respectively. Let $d_{HSI}(p, q)$ denote the distance between these two points.

2.2 Color morphological operators

Based on the measurements of the color distance and the ordering scheme, we can then apply the primary operators of the color mathematical morphology (CMM). The basic operators in the CMM are erosion and dilation operators:

A. Erosion and Dilation

The erosion of image f with an n -sized structure element B on pixel x is defined as:

$$\varepsilon_{CRC}^{nB}(f)(x) = \{f(y) : f(y) = \Lambda_{CRC}[f(z)], z \in n(B_x)\}. \quad (1)$$

Similarly, the dilation of image f with the n -sized structure element \tilde{B} on pixel x can be expressed as:

$$\delta_{CRC}^{nB}(f)(x) = \{f(y) : f(y) = V_{CRC}[f(z)], z \in n(\tilde{B}_x)\}, \quad (2)$$

where Λ_{CRC} and V_{CRC} denote the infimum and supremum according to the proposed CRC-ordering, and \tilde{B}_x denotes reflected structuring element with pixel x .

B. Gradient

The gradient reflects the status of the decline in intensity. The gradient value of a real object boundary is normally larger than that of the internal region of the object. The purpose of the gradient operator is to generate a symbolic energy distribution of the information on the texture of the image. After the dilation operation for image f and after subtracting by the eroded image, the remaining value of the gradient is the norm value, which is

$$\nabla_{CRC}(f) = \|\delta_{CRC}^{nB}(f) - \varepsilon_{CRC}^{nB}(f)\|. \quad (3)$$

In this paper, the gradient extraction acts as a pre-processing of the watershed segmentation.

2.3 A Hybrid ordering algorithm

We proposed a hybrid color ordering method, this not only maintains the merit of R-ordering by reducing the dimension of the feature vector thereby decreasing the computation cost, but it also avoids the ambiguous situation created by C-ordering when measuring the importance of the color vector. In addition, we apply the strategy of automatic reference color selection (ARCS). The CRC-ordering approach is illustrated by using the following three phases.

A. Automatic reference color selection (ARCS) scheme

There is scant if any information in the literature on selecting the reference color c_{ref} . Generally speaking, the major criterion for color selection is to select the pixel that is most distant from the testing color pixel. In short, the most appropriate reference color is selected by using the complementary color of the dominant color. This method provides the distance measure for achieving the highest discriminative ability. The statistical histogram $h(j)$ of image f is obtained by Eq. (4) shows:

$$h(j) = \sum_i \Delta[L_{HSI}(c_i^H, c_i^S, c_i^I) - j], \quad \text{for } 0 \leq j \leq 2^\rho, \forall i \in f \quad (4)$$

where, $\Delta(\cdot)$ denotes the Kronecker delta function (i.e., $\Delta(x) = 1$ for $x = 0$, $\Delta(x) = 0$ otherwise), $L_{HSI}(\cdot)$ denotes the mapping function which enables the 3-dimensional HSI color model to transform as a 16 bits value with 8 bits from the H component, and 4 bits from the S and I components respectively, and ρ denotes the number of bits

mapped from the three components in the HSI color space ($\rho = 16$ in this paper), and j denotes the bin value of the color histogram. The bin with the maximal value then computes the complementary color to serve as the reference color, that is:

$$j^* = \arg_j \max h(j), \quad \text{for } 0 \leq j \leq 2^\rho \quad (5)$$

and

$$c_{ref} = complement(L_{HSI}^{-1}(j^*)), \quad (6)$$

where j^* denotes the bin of the histogram with maximal value , and $L_{HSI}^{-1}(\cdot)$ denotes the reverse mapping function which is used to obtain the HSI color value from the input bin.

B. Global ranking

The R-ordering is a color ranking operation based on the distance between the color of the pixel being tested and the reference color projected onto the color space:

$$c_p <_{c_{ref}} c_q \Leftrightarrow \|c_p - c_{ref}\|_{d_{HSI}}^{HSI} > \|c_q - c_{ref}\|_{d_{HSI}}^{HSI} \quad (7)$$

where c_p and c_q denote two pixels with different color components, $<_{c_{ref}}$ denotes the pixel-based comparison operator with the selected reference color c_{ref} , $\|\cdot\|_{d_{HSI}}^{HSI}$ denotes the HSI distance measurement d_{HSI} , and the superscript HSI means the used color model.

C. Local ranking

The C-ordering is utilized for avoiding an ambiguous situation. For example, if there are two color pixels with different color components in the color space, but the distance from the reference pixel is identical, then the result is that they will be classified as the same color. To prevent this problem, the proposed CRC-ordering algorithm takes the C-ordering method into consideration. This method has also been called lexicographical ordering, and is expressed as,

$$c_p <_{CRC} c_q \Leftrightarrow \begin{cases} \|c_p - c_{ref}\|_{d_{HSI}}^{HSI} > \|c_q - c_{ref}\|_{d_{HSI}}^{HSI} & \text{or} \\ \|c_p - c_{ref}\|_{d_{HSI}}^{HSI} = \|c_q - c_{ref}\|_{d_{HSI}}^{HSI} & \text{and} \\ \begin{cases} c_p^I < c_q^I & \text{or} \\ c_p^I = c_q^I \text{ and } c_p^S < c_q^S & \text{or} \\ c_p^I = c_q^I \text{ and } c_p^S = c_q^S \text{ and } c_p^H < c_q^H \end{cases} \end{cases} \quad (8)$$

where $c_p = (c_p^H, c_p^S, c_p^I)$ and $c_q = (c_q^H, c_q^S, c_q^I)$ represent two with HSI pixel color information.

3 Image Segmentation Based on the CRC-ordering and Quartile Analysis

In this study, the formal procedure of bottom-up image segmentation includes three parts: i) watershed pre-segmentation based on the color gradient image, ii) Region merge using CRC-ordering, and iii) Adaptive threshold determination using quartile analysis.

3.1 Image pre-segmentation

The purpose of this phase is to extract the initial partitions of the image, by adopting the color gradient and the watershed-based segmentation.

The watershed-based algorithm is the one of the most efficient image segmentation methods, and was first presented by Vincent and Soille [27]. The main idea of the watershed algorithm is to consider the original image as a stereo mountain diagram. The gradient energy is treated as the rise and fall of the mountain.

3.2 Region merge using CRC-ordering

Suppose that the initial partitioning of the region is performed by watershed segmentation, and is denoted as $S = (R_1, \dots, R_n)$. The goal of image merging is to achieve a merger discrimination matrix P which represents the result of the final segmentation. We then tag the watershed image as the initial image, and apply the merge step using the bottom-up scenario to do a global search for the two tags (i.e., regions) with the minimum difference. This difference stands for the mean value of the color distance D_g derived from the reference color which uses the dominant color of the whole image (i.e., global rank). If we assume that $R_i = (p_1, \dots, p_n)$ and $R_j = (q_1, \dots, q_m)$ represent the two groups of pixels in the adjacent regions, the global distance for R_i can be computed by,

$$D_g(R_i, c_{ref}^g) = \frac{1}{n} \sum_{k=1}^n d_{HSI}(p_k, c_{ref}^g). \quad (9)$$

where c_{ref}^g can be obtained by Eq. (6) indicating the global reference color, as well as $D_g(R_i, c_{ref}^g)$. According to Eq. (7), the ranking relationship between the two regions of these average color distances can be measured by R-ordering:

$$R_i <_{c_{ref}^g} R_j \Leftrightarrow D_g(R_i, c_{ref}^g) > D_g(R_j, c_{ref}^g) \quad (10)$$

To deal with the drawback of R-ordering creating an ambiguous situation, we applied the C-ordering scheme in this system. From a local viewpoint, we computed the difference value D_l between these two adjacent regions. More specifically, we measured the average color distance using the dominant color as the reference color, that indicates as the dotted brown and green dash lines in Fig.1. It defines as:

$$D_l(R_i, c_{ref}^{R_j}) = \frac{1}{n} \sum_{k=1}^n d_{HSI}(p_k, c_{ref}^{R_j}), \quad (11)$$

where $c_{ref}^{R_j}$ denotes the reference color regarding to region R_j , which can be obtained by Eq. (6).

Based on the Eqs. (10) and (11), the CRC-ordering operation $<_{CRC}^R$ can be derived from:

$$R_i <_{CRC}^R R_j \Leftrightarrow \begin{cases} D_g(R_i, c_{ref}^g) > D_g(R_j, c_{ref}^g) & \text{or} \\ D_g(R_i, c_{ref}^g) \leq D_g(R_j, c_{ref}^g) \text{ and} \\ \{D_l(R_i, c_{ref}^{R_j}) < D_l(R_j, c_{ref}^{R_i})\}. \end{cases} \quad (12)$$

As a result, the merger discrimination matrix P can be constructed using the global threshold TH_g and the local threshold TH_l for the global region distance D_g and the local region distance D_l , that is

$$P(R_i, R_j) = \begin{cases} \text{true} & \text{if } D_g(R_i, R_j) < TH_g \text{ and } D_l(R_i, R_j) < TH_l \\ \text{false} & \text{otherwise.} \end{cases} \quad (13)$$

Finally, the task of the CRC-ordering can be achieved by determining the minimum difference value. When the $D_g(R_i, R_j)$ is less than the global threshold TH_g as well as the $D_l(R_i, R_j)$ is less than the local threshold TH_l , these two regions can be merged. The algorithm terminates when this difference value is larger than a predefined threshold.

As previously mentioned, the CRC-ordering method needs to determine a threshold value for dealing with the region merge. For different images, a specific threshold is required. To solve this problem, we use the quartile analysis method for the adjacent regions and determine a best threshold for merging.

A. Quartile analysis

The quartile analysis is a type of statistical method [28], [29]. The quartiles of a ranked set of data values are the three points that divide the data set into four equal groups. As a result, each group comprises a quarter of the data and distinct by the points on the 25%, 50%, and 75% of the highest value of the data set, which marked as Q_1 , Q_2 , and Q_3 , respectively. Furthermore, the value of $Q_3 - Q_1$ is called as Interquartile range (IQR), which is usually applied for characterizing the data when there may be extremities that skew the data. The IQR is a relatively robust statistic compared to the range and standard deviation, which represents the distribution among 50% data set approaching to the median value. To check the existence of the outliers and determine the “fences”, quartiles can be used to check for outliers via the upper and lower limits of the data. That is, any observation called outlier when it outside the range: $[Q_1 - k(Q_3 - Q_1), Q_3 + k(Q_3 - Q_1)]$, where k denotes a nonnegative constant.

B. Region merge algorithm using the quartile analysis

Based on the quartiles of Q_1 and Q_3 , we analyze the distributions of two neighboring regions R_i and R_j . First, the values of HSI color distance regarding to the reference color c_{ref}^g are viewed as the data set for quartile analysis. Second, we obtain the values of the Q_1 , Q_2 , and Q_3 . Finally, we consider these two regions R_i and R_j whether to merge or not based on observing the value of the IQR.

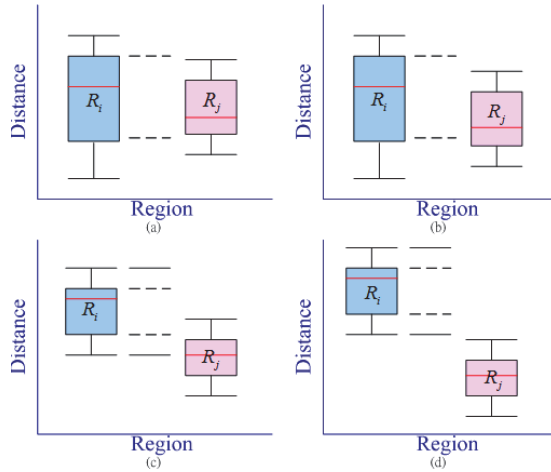


Fig. 1. Quartile analysis to four cases for merge determination, (a)first priority to merge, (b)second priority to merge, (c)third priority to merge, (d) do not merge.

Here, we suppose that the amount of pixels in the R_i is greater than it in the R_j . There are four cases will meet in the quartile analysis (as shown in Fig. 1):

The first case: the HSI distance distribution of the R_j is completely included in the R_i , that is $Q_1^g(R_j, c_{ref}^g) > Q_1^g(R_i, c_{ref}^g)$ and $Q_3^g(R_j, c_{ref}^g) < Q_3^g(R_i, c_{ref}^g)$. It indicates that the color distribution of the R_j belongs to the R_i . In this case, regions R_j and R_i are allowed to merge and assigned a highest priority for region merging, as shown in Fig. 2(a).

The second case: the HSI distance distribution of the R_j is partially included in the R_i , we have

- a) $Q_1^g(R_j, c_{ref}^g) > Q_1^g(R_i, c_{ref}^g)$ and $Q_3^g(R_j, c_{ref}^g) < Q_3^g(R_i, c_{ref}^g)$, or
- b) $Q_3^g(R_j, c_{ref}^g) > Q_1^g(R_i, c_{ref}^g)$ and $Q_3^g(R_j, c_{ref}^g) < Q_3^g(R_i, c_{ref}^g)$.

It shows that a part of the color distribution of R_j is included in R_i . In this case, regions R_j and R_i are enabled to merge with the second priority, as shown in Fig. 1(b).

The third case: the HSI distance distribution of R_j is excluded in R_i . However, the distribution range of R_j still located in the maximum and minimum observation values of the R_i (i.e., 1.5 times of the IQR), it satisfies the following conditions:

- a) $Q_1^g(R_j, c_{ref}^g) > Q_{1-1.5IQR}^g(R_i, c_{ref}^g)$
- b) $Q_1^g(R_j, c_{ref}^g) < Q_{3+1.5IQR}^g(R_i, c_{ref}^g)$

- c) $Q_3^g(R_j, c_{ref}^g) > Q_{1-1.5IQR}^g(R_i, c_{ref}^g)$
- d) $Q_3^g(R_j, c_{ref}^g) < Q_{3+1.5IQR}^g(R_i, c_{ref}^g)$

This denotes that the color distribution of R_j is not belong to R_i , however it remains the tolerant range for R_1 . In this case, regions of R_j and R_i are permitted to merge with third priority, as shown in Fig. 1(c).

The fourth case: the HSI distance distribution range of the R_j is not only completely included in the R_i , but also outside of the maximum and minimum observation values of the R_i (i.e., 1.5 times of the IQR). Therefore, it represents that the pixels in the regions R_j and R_i are completely different set. Referring to the Fig. 1(d), we unable to merge together these two regions in this case.

4 Experimental Results

To evaluate the performance of the proposed method, we used an experimental PC with Intel® Core™ i5 750 CPU, 2.66GHz, and 4GB main memory. The software used was Dev-C/C++ 4.9.9.2 and MATLAB 7.11.0. The testing images were obtained from the Berkeley Segmentation Dataset [30].

We compared the results of the proposed CRC-ordering scheme with other typical approaches in image segmentation application, including the marker-controlled watershed method [31] and the mean-shift clustering method [32]. We considered four standard indexes to evaluate quantitatively flexible evaluate the performance of our proposed method. In this study, four indexes were used to evaluate the quantitative comparison of typical methods, including Normalized probabilistic rand index (NPRI) [33], Variation of Information (VoI) [34], Global Consistency Error (GCE) [35], and Boundary Displacement Error (BDE) [36].

4.1 Experiment 1: Cross-validation of the system sensitivity

In order to analyze the robustness of the system, we verified our image segmentation system reliability with diverse system parameters. Table 1 shows the parameters used in this section. Table 2 presents the experimental results for different parameters in order to illustrate the accuracy of the segmentation. The best performance is achieved when the ARCS is applied in the CRC-ordering method. Moreover, the relatively high inter-channel correlation in RGB color space, results in ranking errors of the vectors. In other words, the segmentation result using the RGB color space frequently acquires the worst performance. Consequently, when the HSI color model is used, it usually performs with consistent results for human perception. It is worth noting that a stronger performance is obtained by the HSI distance measurement than by the Euclidean distance measurement. Fig. 2 shows three testing images, indicating that the validity of the proposed method can achieve a robust performance.

Table 1. The different parameters applied to the CRC-ordering segmentation algorithms

Approaches	ARCS	Distance measure	Color space
The proposed	YES (c_{ref}^g = complement of dominant color)	HSI distance	HSI
Without ARCS	NO (c_{ref}^g = black color)	HSI distance	HSI
Using Euclidean distance	NO (c_{ref}^g = black color)	Euclidean distance	HSI
Using RGB color space	NO (c_{ref}^g = black color)	Euclidean distance	RGB

Table 2. The comparison of different parameters for the CRC-ordering segmentation algorithms

Approaches	Performance Evaluation							
	NPRI [33]		Vol [34]		GCE [35]		BDE [36]	
	Rank1	Rank2	Rank1	Rank2	Rank1	Rank2	Rank1	Rank2
The proposed	120 (40.0%)	279 (93.0%)	96 (32.0%)	285 (95.0%)	12 (4.0%)	91 (30.3%)	119 (39.7%)	293 (97.7%)
Without ARCS	97 (32.3%)	222 (74.0%)	78 (26.0%)	227 (75.7%)	11 (3.7%)	74 (24.7%)	95 (31.7%)	233 (77.7%)
Using Euclidean distance	81 (27.0%)	193 (64.3%)	66 (22.0%)	192 (64.0%)	9 (3.0%)	60 (20.0%)	82 (27.3%)	198 (66.0%)
Using RGB color space	59 (19.7%)	136 (45.3%)	47 (15.7%)	135 (45.0%)	7 (2.3%)	42 (14.0%)	58 (19.3%)	143 (47.7%)

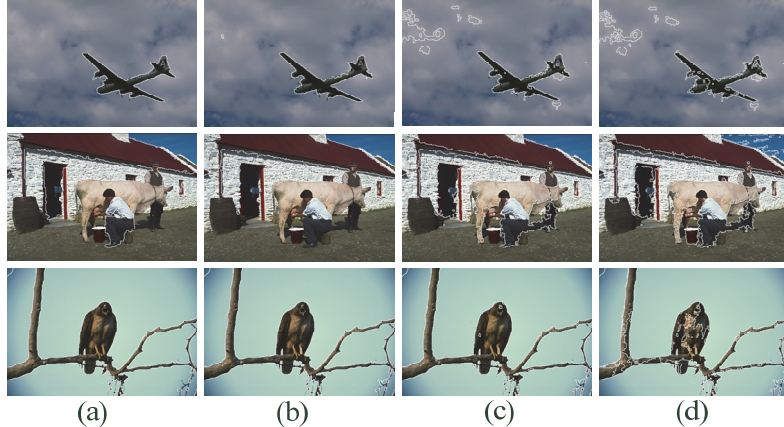


Fig. 2. Image segmentation results with the best thresholds: *airplane*, (a) the proposed CRC-ordering ($TH_l=0.65$), (b) CRC-ordering without ARCS ($TH_l=0.50$), (c) using Euclidean distance($TH_l=0.55$), (d) using RGB color space ($TH_l=0.55$).

4.2 Experiment 2: A comparison with the typical methods

First of all, two state-of-the-art segmentation methods were replicated and used in the evaluation of the system. Table 3 shows the quantitative comparisons. Based on our observation, we chose a unified merger threshold TH_l of 0.65. We tested 300 images from the Berkeley Segmentation Dataset [30]. In Table 3, Rank1 denotes the first

ranked segmentation results, and Rank2 denotes the median rank. Based on the results of the quantitative evaluation shown in Fig. 3. Overall, the performance of the CRC-ordering is moderate, but it is more consistent with the subjective human perception than the mean-shift clustering method, especially in regions with small patches, and rarely suffers from over-segmentation. Regardless of the objective evaluation of the proposed CRC-ordering is not as good as mean-shift clustering method. Nevertheless, the resulting image is obviously inconsistent with human perceptual feelings, and the over-segmented situations being globally reduced.

Table 3. A comparison of different image segmentation algorithms

Algorithms	Performance Evaluations							
	NPRI [33]		VoI [34]		GCE [35]		BDE [36]	
	Rank1	Rank2	Rank1	Rank2	Rank1	Rank2	Rank1	Rank2
CRC-ordering	120(40.0%)	279(93.0%)	96(32.0%)	285(95.0%)	12(4.0%)	91(30.3%)	119(39.7%)	293(97.7%)
Mean-shift clustering [31]	166(55.3%)	278(92.7%)	15(5.0%)	52(17.3%)	74(24.7%)	252(84.0%)	175(58.3%)	295(98.3%)
Marker Watershed [32]	14(4.7%)	43(14.3%)	189(63.0%)	263(87.7%)	214(71.3%)	257(85.7%)	6(2.0%)	12(4.0%)

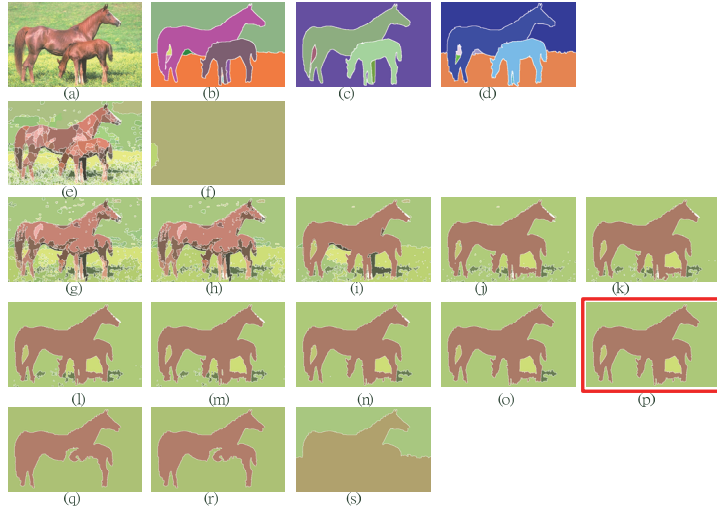


Fig. 3. Image segmentation results: *horse*. (a) Original image, (b)-(d) ground-truth boundary, (e) mean-shift clustering method, (f) Marker Watershed method, (g)-(s) CRC-ordering result for different thresholds (i.e., $TH_l=0.2, 0.25, 0.3, 0.35, 0.4, 0.45, 0.5, 0.55, 0.6, 0.65, 0.7, 0.75, 0.8$), where the best result is $TH_l=0.65$ with red-boxed.

4.3 Experiment 3: A comparison of region merging algorithms

In Section 3.2, we mentioned the region merging algorithm based on the quartile analysis, computing the HSI distance values between the reference colors for two neighboring regions. This method avoids the threshold determination problem of the CRC-ordering method, which replaced by the characteristics of the data cluster to

select a suitable threshold. We apply the mean-shift-based image segmentation method to initially segment images and four indexes are used to evaluate the results of the region-merging algorithms. The proposed quartile-based method is also compared with the other two image segmentation methods.

Based on the result images in Fig. 4, the segmented results of quartile method outperformed to the mean-shift-based and CRC-ordering methods. Perceptually, the results of mean-shift clustering method were over-segmented, whereas the CRC-ordering method was under-segmented. Compared with the ground-truth images, the proposed quartile method achieved the inherent segmentation results. Nevertheless, we received the performance deducing for the VoI and GCE indexes. It was because that the quartile method enabled to avoid the over-segmentation, resulting in the small region was ignored. In addition, we only used the color information. It was difficult to differentiate the foreground and background with the similar color tone simultaneously.



Fig. 4. More comparisons of automatic image segmentation. (1) Original image, (2)-(4) ground truth images, (5) mean-shift clustering method, (6) CRC-ordering method ($TH_l=0.65$), (7) based on quartile analysis.

5 Conclusions

This paper we solved the threshold-sensitive problem when the CRC-ordering scheme applying for region merges. An alternative method based on quartile analysis was proposed and successfully to avoid the CRC-ordering method for an additional threshold determination step. This achieved the region merge simpler and more practical. The HSI distance measurement was employed to determine the rank of the color vectors and to discriminate the merger likelihood between two adjacent regions. Furthermore, the proposed CRC-ordering scheme was applied in cooperation with the automatic reference color selection to deal with the color MM processing.

Acknowledgement. This work is partially supported by Ministry of Science and Technology of Taiwan, under grant NSC102-2221-E-155-037-MY2 and MOST 103-2221-E-155-027-MY2.

References

1. M. Krinidis and I. Pitas, "Color Texture Segmentation Based on the Modal Energy of Deformable Surfaces," *IEEE Transactions on Image Processing*, vol. 18, no. 7, pp. 1613-1622, July 2009.
2. P.F. Felzenszwalb and D.P. Huttenlocher, "Efficient Graph-Based Image Segmentation," *International Journal of Computer Vision*, vol. 59 (2), pp. 167-181, September 2004.
3. H. Permuter, J. Franco, and I. Jermyn, "A study of Gaussian mixture models of color and texture features for image classification and segmentation," *Pattern Recognit.*, vol. 39, no. 4, pp. 695-706, 2006.
4. H. Deng and D. A. Clausi, "Unsupervised Image Segmentation Using a Simple MRF model with A New Implementation Scheme," *Pattern Recognit.*, vol. 37, no. 12, pp. 2323-2335, 2004.
5. J. Chen, T. N. Pappas, A. Mojsilovic, and B. E. Rogowitz, "Adaptive Perceptual Color-Texture Image Segmentation," *IEEE Transactions on Image Processing*, vol. 14, no. 10, pp. 1524-1536, Oct. 2005.
6. Y. Deng and B. S. Manjunath, "Unsupervised segmentation of color-texture regions in images and video," *IEEE Trans. Pattern Anal. Mach. Intell.*, vol. 23, no. 8, pp. 800-810, Aug. 2001.
7. E. Saber, A. Tekalp, and G. Bozdagi, "Fusion of color and edge information for improved segmentation and edge linking," *Imag. Vis. Comput.*, vol. 15, no. 10, pp. 769-780, Jan. 1997.
8. D. E. Ilea and P. F. Whelan, "CTex—An Adaptive Unsupervised Segmentation Algorithm Based on Color-Texture Coherence," *IEEE Transactions on Image Processing*, vol. 17, no. 10, pp. 1926-1939, Oct. 2008.
9. L. G. Ugarriza, E. Saber, S. R. Vantaram, V. Amuso, M. Shaw, and R. Bhaskar, "Automatic Image Segmentation by Dynamic Region Growth and Multiresolution Merging," *IEEE Transactions on Image Processing*, vol. 18, no. 10, pp. 2275-2288, Oct. 2009.
10. J. Shi and J. Malik, "Normalized cuts and image segmentation," *IEEE Trans. Pattern Anal. Mach. Intell.*, vol. 22, no. 8, pp. 888-905, Aug. 2000.
11. D. E. Ilea and P. F. Whelan, "Image Segmentation based on the Integration of Colour-texture descriptors—A review," *Pattern Recognit.*, vol. 44, no. 10-11, pp. 2479-2501, Oct. 2011.
12. O. Severino Jr. and A. Gonzaga, "A new approach for color image segmentation based on Color Mixture," *Machine Vision and Appl.*, vol. 24, no. 3, pp. 607-618, April 2013.
13. J. Angulo and J. Serra, "Modeling and Segmentation of colour images in polar representations," *Image Vis. Comput.*, vol. 25, no. 4, pp. 475-495, 2007.
14. V. Patrascu, "New fuzzy color clustering algorithm based on hsl similarity," in: *World Congress and 2009 European Society of Fuzzy Logic and Technology Conference*, Lisbon, Portugal, 2009, pp. 48-52.
15. T. Randen and J. H. Husoy, "Filtering for texture classification: A comparative study," *IEEE Trans. Pattern Anal. Mach. Intell.*, vol. 21, no. 4, pp. 291-310, Apr., 1999.

16. W.-Y. Ma and B. S. Manjunath, "EdgeFlow: A Technique for Boundary Detection and Image Segmentation," *IEEE Transactions on Image Processing*, vol. 9, no. 8, pp. 1375-1388, Aug. 2000.
17. T. Chang and C.-C. J. Kuo, "Texture analysis and classification with tree-structured wavelet transform," *IEEE Transactions on Image Processing*, vol. 2, no. 4, pp. 429-441, Oct. 1993.
18. E. Aptoula, S. Lefèvre, "On the morphological processing of hue," *Image and Vision Computing*, vol. 27, no. 9, pp. 1394-1401, August 2009.
19. E. Aptoula, S. Lefèvre, "A comparative study on multivariate mathematical morphology," *Pattern Recognition*, vol. 40, no. 11, pp. 2914-2929, November 2007.
20. J. Angulo, "Unified morphological color processing framework in a lum/sat/hue representation," in: *International Symposium on Mathematical Morphology (ISMM'05)*, 2005, pp. 387-396.
21. C. Zhao, "A new vectorial ordering for color morphology based on marginal ordering," in: *The 5th International Conference on Computer Science & Education (ICCSE'10)*, Hefei, China, August 2010, pp. 1769-1772.
22. R. Lukac, B. Smolka, K. Martin, K.N. Plataniotis and A.N. Venetsanopoulos, "Vector Filtering for Color Imaging," *IEEE Signal Processing Magazine*, vol. 22, no. 1, pp. 74-86, Jan. 2005.
23. E. Aptoula , S. Lefèvre, "On lexicographical ordering in multivariate mathematical morphology," *Pattern Recognition Letters*, vol. 29, no. 2, pp. 109-118, January 2008.
24. A.N. Evans, "Nonlinear Operations for Colour Images Based on Pairwise Vector Ordering," in: *Proceedings of the Digital Imaging Computing: Techniques and Applications (DICTA'05)*, December 2005, pp.61.
25. J. Angulo, "Morphological colour operators in totally ordered lattices based on distances: Application to image filtering, enhancement and analysis," *Computer Vision and Image Understanding*, vol. 107, no. 1-2, pp. 56–73, July 2007.
26. L. Wang, Y. Zhang and J. Feng, "On the Euclidean Distance of Images," *IEEE Transactions on Pattern Analysis and Machine Intelligence*, vol. 27, no. 8, pp. 1334-1339, August 2005.
27. L. Vincent, P. Soille, "Watersheds in Digital Spaces: An Efficient Algorithm Based on Immersion Simulations," *IEEE Transactions on Pattern Analysis and Machine Intelligence*, vol. 13, no 6, pp. 583-598, June 1991.
28. R. J. Hyndman and Y. Fan, "Sample quantiles in statistical packages," *American Statistician*, vol. 50, pp. 361-365, 1996.
29. R. Kara-Falah, P. Bolon, J.P. Cocquerez, "A region-region and region-edge cooperative approach of image segmentation," in *Proc. ICIP*, vol.3, 1994, pp.470-474.
30. Berkeley Segmentation Dataset [Online]: <http://www.eecs.berkeley.edu/Research/Projects/CS/vision/bsds/> (latest access time January 22,2014)
31. K. Parvati, B.S. Prakasa Rao, and M. Mariya Das, "Image Segmentation Using Gray-Scale Morphology and Marker-Controlled Watershed Transformation," *Discrete Dynamics in Nature and Society*, 2008, doi:10.1155/2008/384346.
32. D. Comanicu and P. Meer, "Mean shift: A robust approach toward feature space analysis," *IEEE Transaction on Pattern Analysis and Machine Intelligence*, vol. 24, no. 5, pp. 603-619, May 2002.
33. R. Unnikrishnan, C. Pantofaru, and M. Hebert, "Toward objective evaluation of image segmentation algorithms," *IEEE Trans.Pattern Anal. Mach. Intell.*, vol. 28, no. 6, pp. 929-944, Jun. 2007.

34. M. Meila, "Comparing Clusterings-An axiomatic view," in *Proc. 22nd Int. Conf. Machine Learning*, 2005, pp. 577-584.
35. D. Martin, C. Fowlkes, D. Tal, and J. Malik, "A database of human segmented natural images and its application to evaluating segmentation algorithms and measuring ecological statistics," in *Proc. 8th Int. Conf. Computer Vision*, Jul. 2001, vol. 2, pp. 416-423.
36. J. Freixenet, X. Munoz, D. Raba, J. Marti, and X. Cufi, "Yet another survey on image segmentation: Region and boundary information integration," in *Proc. 7th Eur. Conf. Computer Vision Part III, Copenhagen, Denmark*, May 2002, pp.408-422.